THE SHAFT RESISTANCE OF DRIVEN PILES IN CLAY

BY

D.M. POTTS and J.P. MARTINS

(Imperial College London)

1. INTRODUCTION

In recent years much research effort has been devoted to the development of an effective stress approach to pile design in clays. Although the objectives of such research are simple the problem has proved to be of such complexity that only limited progress has been made to date. The major problems arise in the prediction of the changes in effective stresses which occur as a result of both installation and the subsequent loading. Much recent work (eg. Randolph et.al. 1979, Kirby and Esrig 1980) has concentrated on predicting stress changes arising from the installation of, and subsequent consolidation around, driven piles in clay. Much progress has been made in this respect. However the same attention has not been given to the effects of loading such piles after installation.

The shaft resistance of a pile may be determined by integration of the shear stresses at failure acting over its surface area in contact with the surrounding soil. The peak (maximum) shear stress τ_{max} acting on the pile shaft may be related to the effective radial stress σ_r' by the following equation,

$$\tau_{max} = \sigma_r' . \tan\delta' + c' \qquad (1)$$

where σ'_r is the radial stress acting at peak shear stress,
δ' represents the peak mobilised angle of friction along the pile shaft,
and c', the effective cohesion intercept; this is usually neglected on account of the remoulding assumed to occur during pile installation.

Thus, in order to estimate the maximum shear stress, the design engineer must be able to predict the values of both σ'_r and δ' acting at peak. These values are likely to be influenced by, among other factors, the soil type, its stress history, the type of pile, the method of pile installation and the rate of loading. Clearly this is a complex situation.

In this paper the results of a numerical investigation into the mobilisation of shear resistance along the shaft of a full displacement pile are presented. The analysis has considered the behaviour of the soil around a short segment of a very long pile, well away from the influences of both the pile tip and the ground surface. The pile is assumed to have been installed by driving and only loaded after any excess pore pressures have dissipated. The stress conditions prevailing in the soil after pile driving and subsequent consolidation have been taken from Randolph et.al. 1979 and Wroth et.al. (1980). The numerical analysis has been performed using the Finite Element method and the soil has been assumed to be an elasto-plastic material behaving in accordance with a form of the Modified Cam Clay model (Roscoe and Burland, 1968).

The behaviour of two piles, one installed in a normally consolidated clay and the other in a clay with an original overconsolidation ratio of eight, will first be discussed. It will be shown that the pile behaviour on loading is essentially controlled by the stress state of the soil immediately adjacent to the pile shaft. The results of a parametric study are then briefly described. The aim of the study was to identify the features of the stress state around the pile after driving and consolidation, to which the subsequent loading behaviour is most sensitive.

2 FINITE ELEMENT ANALYSIS

For the purposes of the present analyses a thin horizontal slice of soil of considerable lateral extent compared to the pile diameter has been considered with boundary conditions relevant to the idealised situation of a long pile in an infinite soil medium. The geometry adopted is illustrated in figure 1, and consists of a horizontal disc of soil having a thickness of 5 units and an external radius of 345 units. The modelled pile of 7.5 units radius is coaxial with the disc. In figure 1 this disc has been divided into 20, eight noded, isoparametric elements. Immediately adjacent to the pile shaft the elements have a width of only 0.25 units.

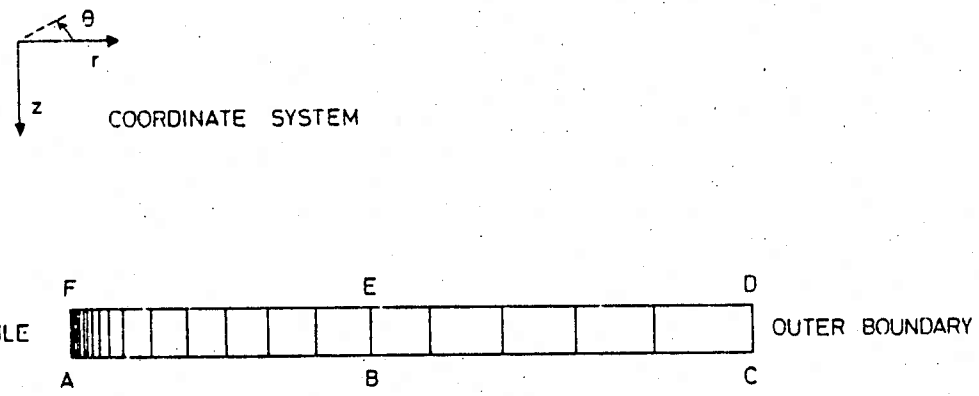

Figure 1: Finite element mesh

To model the loading of the pile axial displacements have been imposed over the boundary AF. To model the infinite extent of the disc zero displacement boundary conditions were imposed over the boundary region CD. Parametric studies were performed varying the element sizes, the number of elements and the radial distance to the boundary CD in order to verify that the mesh shown in figure 1 accurately modelled the problem under consideration. Along the boundaries AC and FD the displacements were tied; that is to say at any radius r the displacements both vertically and radially at corresponding nodes on AC and FD were forced to be identical. This resulted in a vertical line such as EB in figure 1 remaining vertical during loading. The magnitudes of both the vertical and radial displacements of this line are clearly unknown at the outset of the calculation and are a result of the analysis. This tying of

displacements was achieved in the finite element analysis by giving the same degree of freedom number to nodes at the same radius along AC and FD. This also resulted in a smaller stiffness matrix and essentially reduced the problem to a one dimensional situation in which all variables were a function of radius only. Initial stresses, equal to the stresses after pile installation and subsequent consolidation, were specified in the soil at the start of the analysis. Pile displacements were applied incrementally and the finite element equations solved using an accelerated form of the initial stress approach. Typically fifty increments of pile displacement were employed with an average of four iterations per increment. A parametric study was performed to ensure that the increment size was sufficiently small to provide accurate predictions.

3 SOIL MODEL

The soil model adopted for the finite element calculations was a form of the Modified Cam Clay model of Roscoe and Burland (1968). In this model it is assumed that the consolidation characteristics of the soil may be adequately represented in $v-\ln(p')$ space by the virgin consolidation line;

$$v = v_1 - \lambda.\ln(p') \qquad (2)$$

and the family of swelling lines;

$$v = v_s - \kappa.\ln(p') \qquad (3)$$

where v=specific volume=1+e, $p' = 1/3(\sigma_r' + \sigma_\theta' + \sigma_z')$ =the mean effective stress, λ is the slope of the virgin consolidation line, κ is the slope of the swelling lines and v_1 is the virgin consolidation specific volume at unit pressure. λ, κ and v_1 are material properties.

Behaviour under increasing deviator stress is assumed to be elastic until a yield curve of the form;

$$F = S^2 - (p_o'/p' - 1) = 0 \qquad (4)$$

is reached at which point strain hardening/softening plastic behaviour occurs. In the above expression p_o' is the value of p' at the intersection of the current swelling line and the virgin consolidation line and S is defined as;

$$S=J/(p'.g(\theta)) \qquad (5)$$

where J the second invariant of the effective stress tensor is defined by $J^2=1/6((\sigma_1'-\sigma_2')^2+(\sigma_2'-\sigma_3')^2+(\sigma_3'-\sigma_1')^2)$, θ=Lode angle (see figure 2), and the function $g(\theta)$ expresses the manner in which the yield surface varies with the Lode angle. In the present studies $g(\theta)$ is taken as either:-
a Mohr Coulomb hexagon given by;

$$g(\theta)=\sin\phi'/(\cos\theta + 1/\sqrt{3}.\sin\theta.\sin\phi') \qquad (6)$$

and where ϕ' is the Mohr Coulomb angle of shearing resistance, or as a circle with;

$$g(\theta)=M/\sqrt{3} \qquad (7)$$

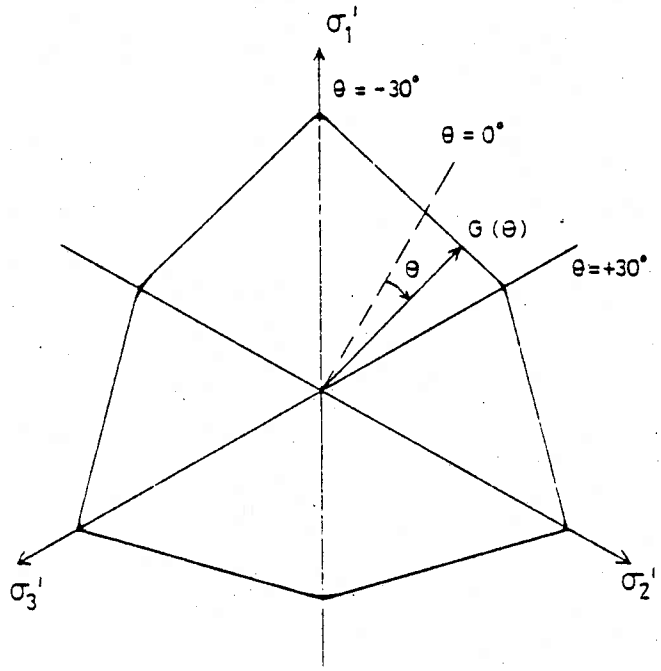

Figure 2: Variation of g(θ) in deviatoric plane

Equation 4 plots as an ellipse, in terms of p' and J above each swelling line given by equation 2 and the major axis of the ellipse is a function of p'_o which varies with v in accordance with equation 2. The intersection of the yield surface with a deviatoric plane produces either a Mohr Coulomb hexagon as described by equation 6 or a circle with radius $M/\sqrt{3}$.

The plastic strain increment vector is assumed to be perpendicular to a plastic potential surface which is also given by equation (4). However, the plastic potential is assumed to be independent of the Lode angle θ having rotational symmetry about the space diagonal in effective stress space. It is therefore obtained from equation 4 by replacing the variable θ, used to evaluate S, by the parameter $\theta(\underline{\sigma}')$, the Lode angle at the point in stress space at which the plastic potential is to be employed to evaluate the plastic strain increments. Although replacing θ by $\theta(\underline{\sigma}')$ does not change the value of F it does change the value of the derivatives of F required to evaluate the strain increments. The intersection of the plastic potential with a deviatoric plane produces a circle. As the pile problem under investigation has a zero strain constraint in the 'z' direction and as the plastic potential has rotational symmetry the stress state at peak load conditions corresponds to a Lode angle $\theta=0^o$, see Potts and Gens (1982). This condition ($\theta=0^o$) will be referred to as the "plane strain" situation throughout the remainder of this paper. In terms of the nomenclature of classical plasticity the yield surface and its plastic potential are non-associated if equation 6 is used to define $g(\theta)$, and associated if equation 7 is employed.

Soil behaviour under unloading and reloading of the effective stress p' is assumed to obey equation 3 which gives the elastic bulk modulus K_B as ;

$$K_B = v.p'/\kappa \qquad (8)$$

This expression indicates that the elastic bulk modulus depends on the stress level p' and the specific volume v. In the original version of Modified Cam clay (Roscoe and Burland, 1968) elastic shear strains were neglected; however, if the model is to be incorporated into an elasto-plastic finite element formulation neglect of elastic shear

strains produces problems when purely elastic behaviour is considered. To overcome this difficulty a constant value of the shear modulus G, independent of stress level, has been adopted.

To completely specify the soil model, values of the following five parameters are required: G, M or ϕ , λ , K and v_1.

4 DRIVEN PILES

Recently considerable research effort into the prediction of likely stress changes occurring in the soil due to pile driving and subsequent consolidation has been made at Cambridge University (e.g. Randolph et.al., 1979)

This work is based on cavity expansion theory incorporating the Modified Cam clay model and employing the finite element method to obtain numerical predictions. One of the most important predictions arising from this research is that after driving and subsequent consolidation the soil adjacent to the pile is in a normally consolidated state, irrespective of its overconsolidation ratio prior to pile installation. The analysis also shows that immediately adjacent to the pile shaft $\sigma_r = Ko_{nc} . \sigma_z$ and $\sigma_\theta = \sigma_z$ where Ko_{nc} is the "at rest" coefficient of earth pressure associated with a one dimensionally normally consolidated clay.

In an attempt to examine the likely stress changes that may arise on subsequent pile loading the results of two of the analyses presented by Randolph et.al. (1979) and Wroth et.al. (1980) were used as initial conditions in numerical calculations using the finite element mesh given in figure 1. The two cases selected were that of a pile installed in an initially normally consolidated Boston Blue Clay and that of a pile installed in London clay having an initial overconsolidation ratio of eight. As a form of the Modified Cam clay model which had rotational symmetry in the deviatoric plane was adopted in the cavity expansion analysis, the model described in section 3 with $g(\theta)=M/3$ has been used for the present calculations. This ensures some form of consistency.

i) Pile Installed in Normally Consolidated Boston Blue Clay

The soil parameters for the Modified Cam clay model were assigned the following values apparently representative of Boston Blue clay;

$$M=1.2,\ \lambda=0.15,\ K=0.03,\ G=12000 KN/m^2,\ v_1=2.83$$

The variation of the principal effective stresses σ_r', σ_z' and σ_θ' with radial distance from the pile, obtained from Randolph et.al. (1979), were input as initial stresses and the soil assumed to be everywhere in a normally consolidated condition. Pile loading was simulated by applying increments of shaft displacement and the analysis performed first under fully drained conditions. The resulting stress path for a soil element adjacent to the pile shaft predicted by the analysis is shown in figure 3 as the dashed line BC_1.

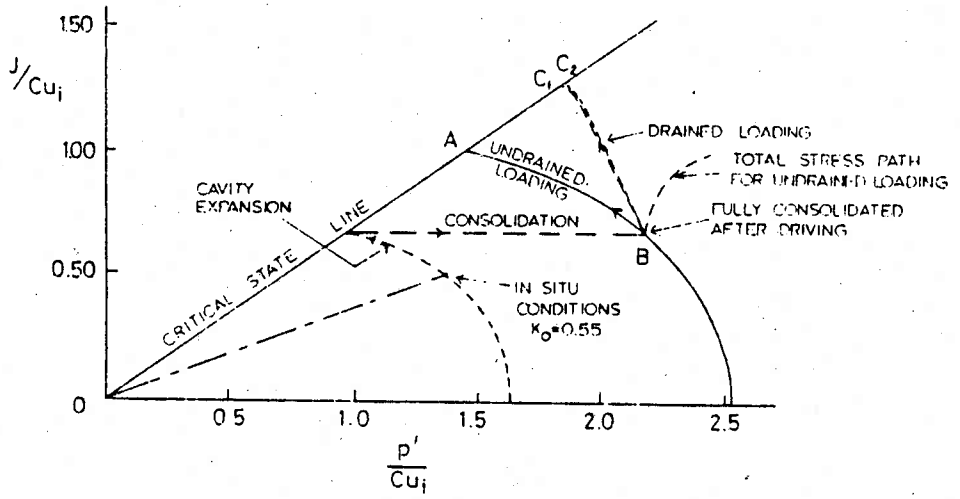

Figure 3: Stress path for a soil element immediately adjacent to a pile installed in normally consolidated Boston Blue clay

Inspection of this figure indicates that the effective stress path followed during the loading travels to the left with a consequent reduction in the mean effective stress p'. The variations with pile displacement of σ_r', σ_θ', σ_z', τ_{rz}, J, γ_{rz} and α for a soil element adjacent to the pile shaft are shown in figure 4. α is defined as the inclination of the maximum principal stress to the z direction.

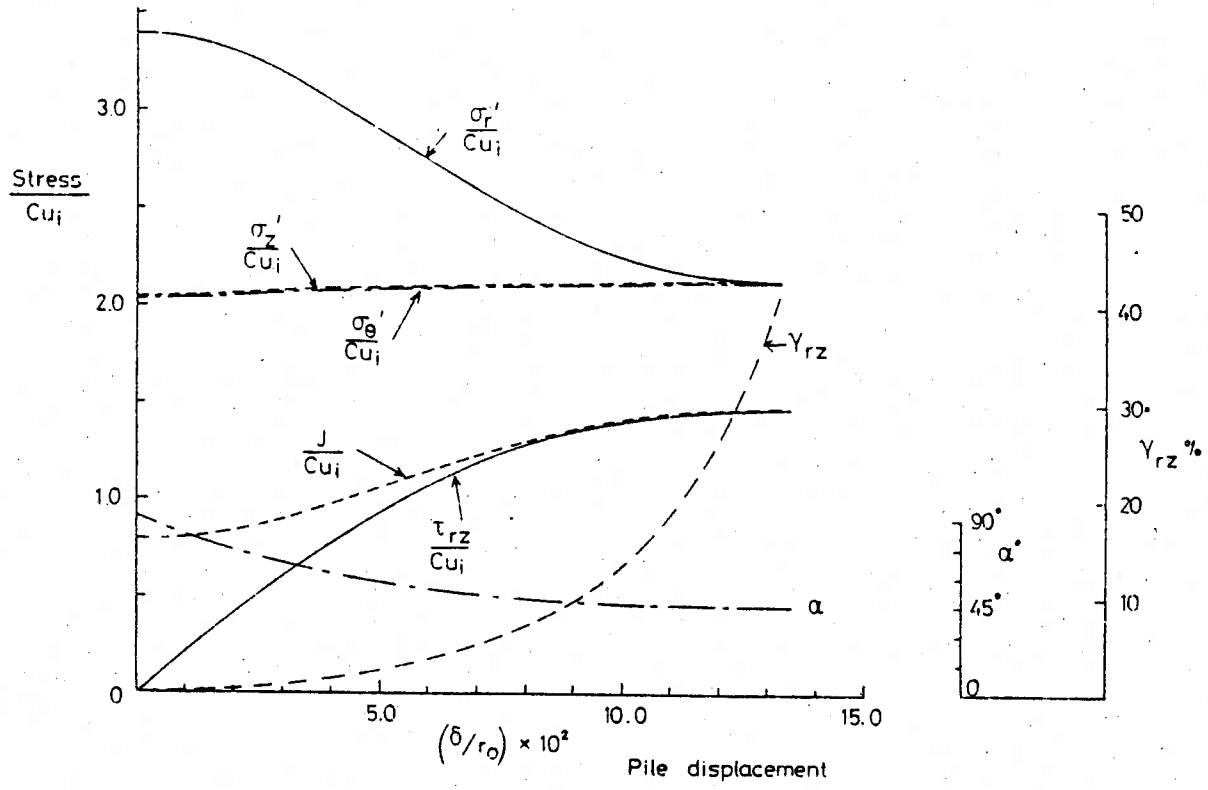

Figure 4: Variation of stresses adjacent to a pile installed in normally consolidated Boston Blue clay on drained loading

In these plots the stresses have been normalised by Cu_i, the undrained shear strength under "plane strain" conditions ($\theta=0^o$), prior to pile loading. The very large reduction in σ'_r (about 40%) during pile loading should be noted. Initially the principal stresses rotated rapidly with pile displacement and after 80% of the peak shaft resistance had been mobilised, the principal stresses had rotated through 40^o of the overall 45^o. At peak the inclination of the major principal stress to the vertical, α, was 45^o indicating that $\delta' = \tan^{-1}(\sin\phi')$, where ϕ' is the equivalent angle of shearing resistance at peak conditions.

The analysis was repeated under undrained conditions and the total stress path for a soil element adjacent to the pile shaft is shown in figure 3. The variations with pile displacement of σ'_r, σ'_z, σ'_θ, τ_{rz}, γ_{rz}, J, u and α in this same soil element are presented in figure 5. In these figures u is the excess pore pressure generated during pile loading. The predicted pore pressure distribution with radius at peak conditions is represented in figure 6.

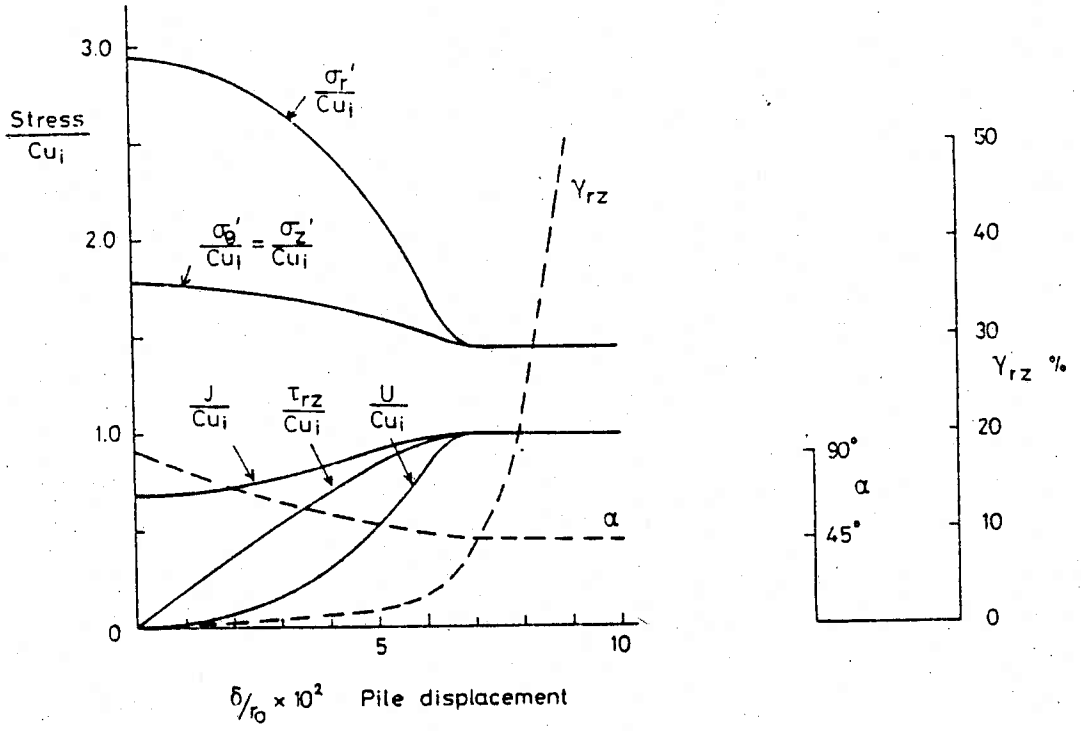

Figure 5: Variation of stresses adjacent to a pile installed in normally consolidated Boston Blue clay on undrained loading

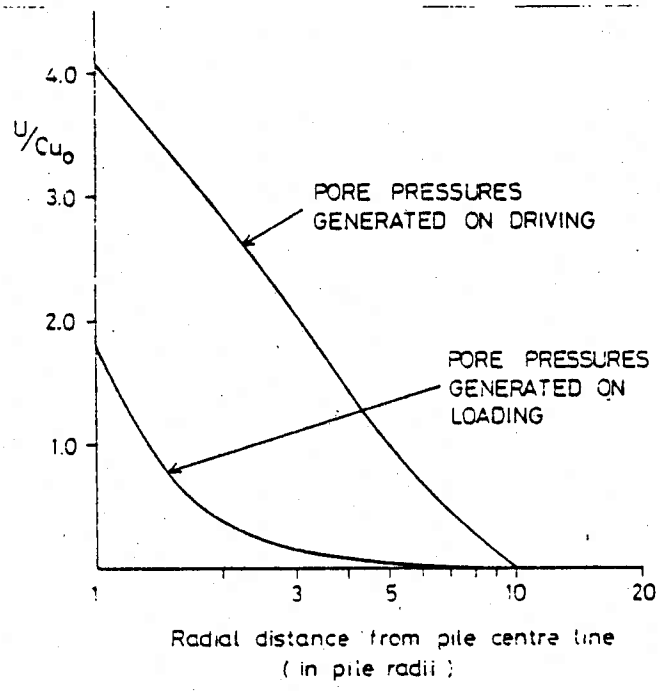

Figure 6: Pore pressure variation with radius

In this figure the pore pressures have been normalised with respect to the undrained shear strength Cu_o prior to pile installation and the radial distance normalised with respect to the pile radius,

and plotted on a logarithmic scale. Also indicated on the figure are the predicted pore pressures generated during pile driving (Randolph et.al. 1979). Inspection of the figure indicates that during pile loading the pore pressures are considerably smaller in magnitude and much more localised than those generated on driving. The times for complete dissipation of pore pressures generated on loading are therefore likely to be quite short compared with the "set up" time and the question arises as to whether pile loading is, in practice, a drained or an undrained phenomenon.

ii) Pile Installed in Overconsolidated London Clay

The soil parameters for the Modified Cam Clay model were assigned the following values;

$$M=0.568,\ \lambda=0.161,\ K=0.062,\ G=6750\ KN/m^2,\ v_1=2.759$$

The variation of the principal effective stresses σ_r', σ_z' and σ_θ', and the undrained shear strength after pile driving and subsequent consolidation were obtained from Wroth et.al.(1980). Pile loading was again simulated by applying increments of shaft displacement and the analysis performed under fully drained conditions. The predicted stress path for a soil element adjacent to the pile shaft is shown in figure 7 as the dashed line BC .

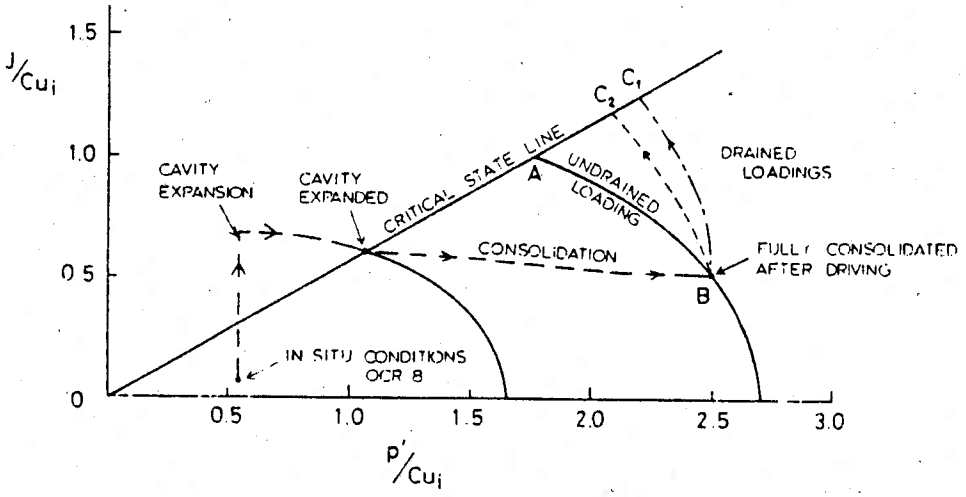

Figure 7: Stress path for a soil element adjacent to a pile installed in over consolidated London clay

The variations of σ_r', σ_z', σ_θ', τ_{rz}, γ_{rz}, α and J for a soil element adjacent to the pile shaft, with pile displacement, are shown in figure 8, the early rapid rotation of principal stresses and the fact that at failure $\alpha = 45^\circ$ should be noted.

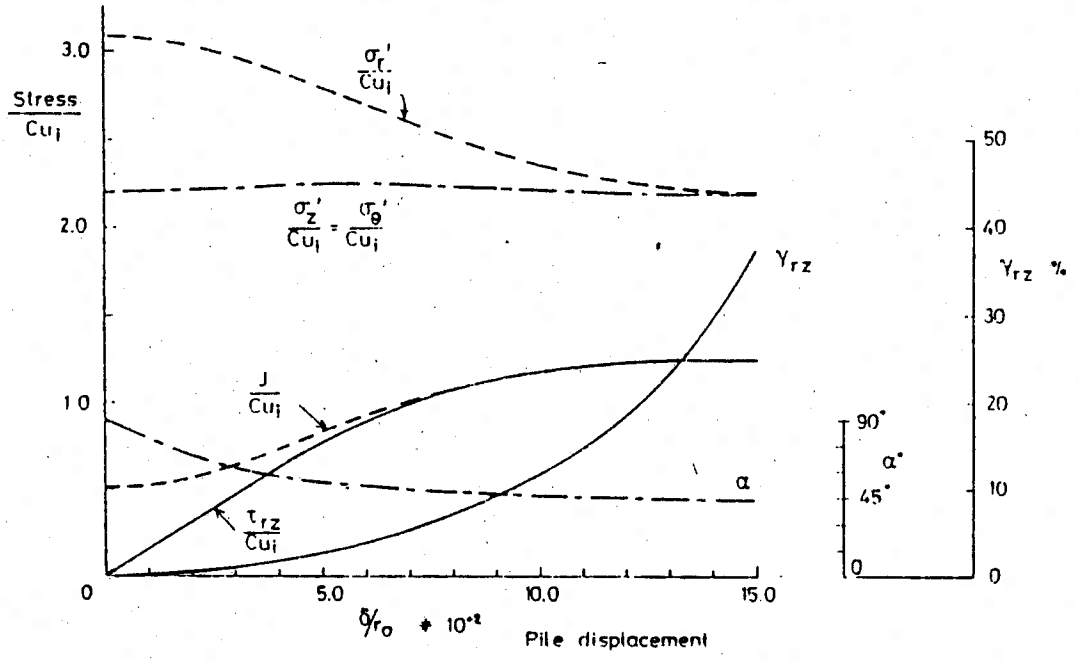

Figure 8: Variation of stresses adjacent to a pile installed in overconsolidated London clay on drained loading.

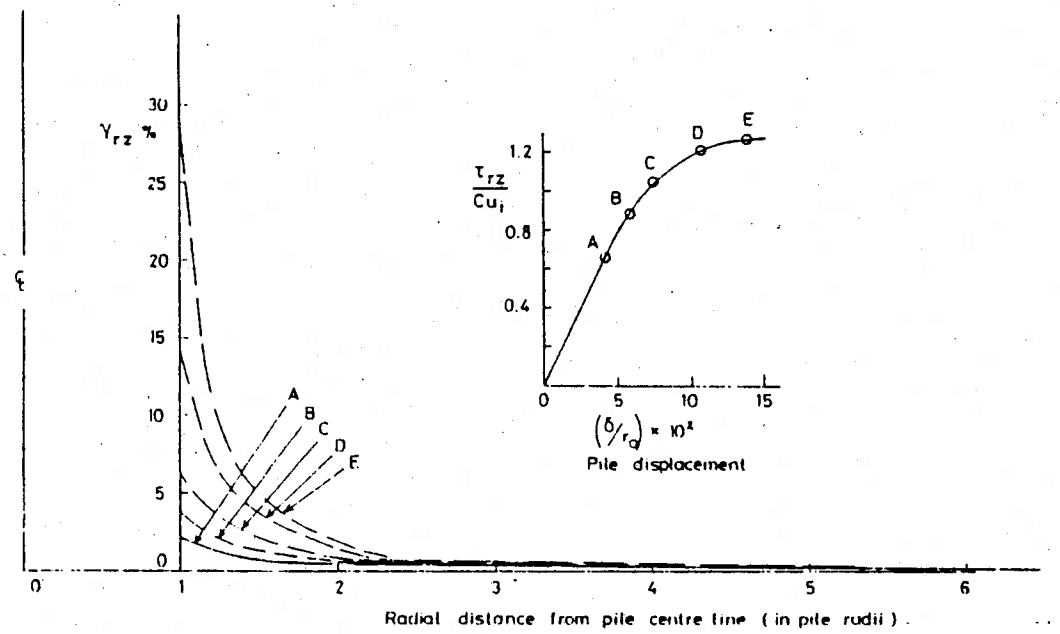

Figure 9: Variation of shear strain with radius

In figure 9 the predicted variations of shear strain γ_{rz} with radial distance from the pile shaft are shown for various stages of loading. From this figure it is evident that as peak conditions are approached, extremely high shear strains are predicted in the immediate vicinity of the pile. If the soil model were to incorporate even very gradual strain softening then progressive failure would be predicted.

iii) Simplified Stress Conditions

Two further analyses were then performed ignoring the radial variation of stresses following pile installation as predicted by Randolph et.al.(1979), and Wroth et.al.(1980). Instead the initial stresses were everywhere set to the values appropriate to the soil immediately adjacent to the pile shaft. The predicted stress path for an element adjacent to a pile driven and then loaded in normally consolidated Boston Blue Clay, is shown as the dotted line BC_2 in figure 3. Inspection of this figure indicates that there is very close agreement between this stress path and that obtained from the previous analysis using the 'correct' initial stress distribution in the soil.

The predicted stress path from a similar analysis of a pile in overconsolidated London Clay is shown as the dotted line BC_2 in figure 7. The close correspondence between this stress path and that obtained using the 'correct' initial stress distribution is not as good as that for the pile installed in normally consolidated material but still illustrates the dominating influence of the material closest to the pile. The approximate analysis predicted a stress path to the left of the 'correct' one and is therefore on the conservative side.

In the cases of the pile installed in both the normally and overconsolidated material, the variations of σ_r, σ_z, σ_θ, τ_{rz}, γ_{rz}, α and J for the soil element adjacent to the pile shaft, with pile displacement, predicted using the simplified initial stresses were also in good agreement with the corresponding analyses employing the 'correct' stresses. It should be noted that in both cases considered the soil immediately adjacent to the pile was taken to be normally consolidated; see Randolph et.al.(1979).

iv) Undrained Behaviour

Analyses employing the simplified stress conditions were performed enforcing undrained conditions. The results were compared with those obtained above for the case of the undrained loading of a pile driven into normally consolidated Boston Blue Clay (employing the 'correct' radial variation of post installation stresses). The main conclusions were that:-

i) the stress state in the element immediately adjacent to the pile shaft controls the pile behaviour on loading.

ii) at peak conditions :-

a) $\sigma'_r = \sigma'_\theta = \sigma'_z$

b) $\alpha^r = 45^o$

c) $\delta' = \tan^{-1}(\sin\phi'_{PS})$

iii) as the loading is undrained , $\tau_{max} = Cu_i$, the undrained shear strength in "plane strain" prior to pile loading.

If the conclusion from Randolph et.al.(1979), that the material adjacent to a driven pile is always normally consolidated is adopted in conjunction with the above observations then the following expression for the reduction of σ'_r on pile loading may be derived:-

$$\frac{\Delta\sigma'_r}{\sigma'_{ri}} = 1-1/3.(1+2Ko_{nc})\left[0.5\left[\left[\frac{3(1-Ko_{nc})}{q(\theta)_{TC}(1+2Ko_{nc})}\right]^2+1\right]\right]^{(1-K/\lambda)}$$

This relationship indicates that the change in the radial effective stress σ'_r , is a function of its initial value after installation (σ'_{ri}) , the magnitude of Ko_{nc} , and the value of $q(\theta)$ prior to loading (adjacent to the pile conditions correspond to triaxial compression ($\theta=-30^o$)). The value of $q(\theta)$ may be determined from equations 6 or 7.

In figure 10 the variation of σ'_r is plotted against Ko_{nc} employing the parameters for London Clay used above, and a Mohr Coulomb hexagon for $q(\theta)$. For values of Ko_{nc} in the range of interest (0.5 to 0.75), the reduction in σ'_r is about 40%. See section 5ii for a further discussion of the effects of the magnitude of Ko_{nc}.

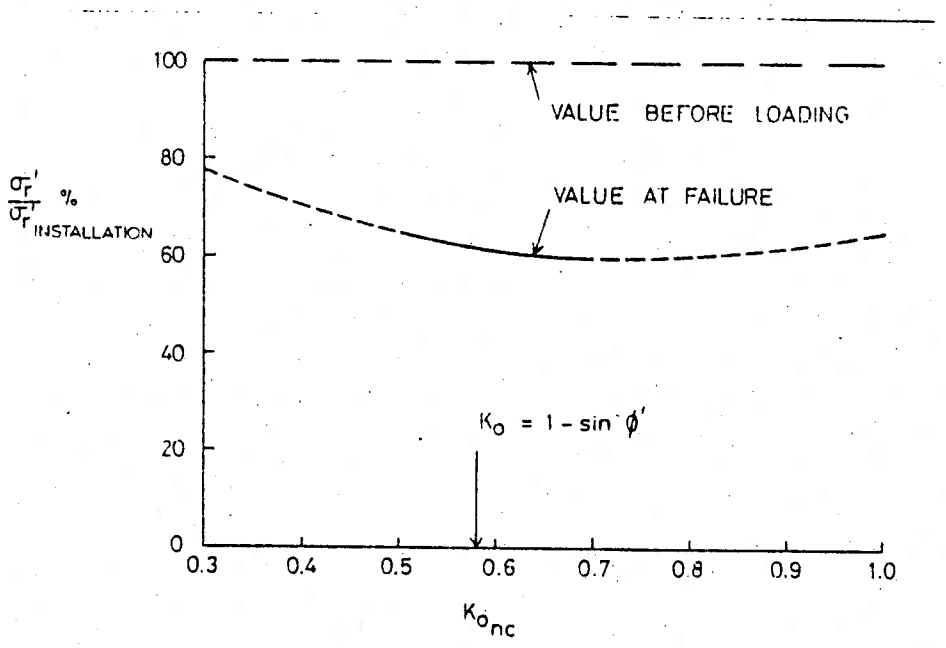

Figure 10: Variation of radial stress on loading as a function of $K_{o_{nc}}$

It is therefore possible to determine the undrained failure conditions without performing a numerical analysis and the undrained case therefore becomes trivial. However, the behaviour under drained conditions is much more complex, and no such simple relations have been found to determine the conditions at peak. In the remainder of this paper, attention is therefore concentrated on drained behaviour. In practice pile loading will probably be a partially drained phenomenon and the actual behaviour would be expected to lie between the bounds of fully drained and undrained conditions.

5 PARAMETRIC STUDY

Apart from the assumptions incorporated in the soil model and the values assigned to the parameters necessary to define it, the above calculations are dependent on the stress state within the soil prior to pile loading. These stresses having been taken directly from the results of cavity expansion analyses. In an attempt to investigate the influence of small perturbations to these values on the pile behaviour on loading, a limited parametric study has been completed. In particular the effects of the shape of the yield curve in the deviatoric plane, the value of $K_{o_{nc}}$ and state of consolidation

immediately adjacent to the pile prior to pile loading have been considered. For the purposes of this study the idealised situation in which the initial stresses do not vary with radius has been employed. A brief discussion of the results of this study will now be given.

i) Shape of the Yield Surface in the Deviatoric Plane

In order to maintain compatibility with the cavity expansion analyses, the calculations performed in the previous sections have adopted a surface of revolution for the yield surface in the deviatoric plane. However, it should be noted that the use of such an assumption leads to a variation of the angle of shearing resistance ϕ' with Lode angle. For example if a value of ϕ' of 25° is specified for triaxial compression ($\theta=-30^\circ$) a value of $\phi = 34.5^\circ$ is obtained in "plane strain" ($\theta=0^\circ$) . Alternatively if $\phi=25^\circ$ is specified at "plane strain" a value of $\phi=19^\circ$ is obtained in triaxial compression. Neither of these two situations is realistic and the majority of clays have ϕ' values which vary little with Lode angle, having, perhaps only a 1° or 2° variation of ϕ' between triaxial compression and "plane strain" conditions.

In order to demonstrate the effect of the shape of the yield surface on the predicted pile behaviour the results of three analyses are presented. All three analyses had the same starting stresses and soil conditions. Two of the analyses have adopted a surface of revolution (SR) for the yield surface (circle in the deviatoric plane) having M values of 0.73 and 0.98 respectively. These M values give ϕ' values in triaxial compression ($\theta=-30^\circ$) of 19° and 25° and at "plane strain" ($\theta=0^\circ$) of 25° and 34.5° respectively. In the third analysis a Mohr Coulomb hexagon has been adopted for the shape of the yield surface in the deviatoric plane (see section 3), and ϕ' has been set to 25°. The resulting stress paths obtained from these analyses are presented in figure 11 and the predicted reduction in σ_r in figure 12. In all cases, as with the previous analyses, the Lode angle $\theta=0^\circ$ and $\sigma_r = \sigma_z = \sigma_\theta$ at peak loading conditions. Considering the two analyses in which a surface of revolution was adopted (curves a and b in figures 11 and 12) the following points should be noted.

i) The predicted values of J at peak conditions are markedly different. However, the values of p' are similar. This results in the peak value of J being directly proportional to the M values adopted in the analysis. As $\alpha = 45^{o}$ at peak conditions in both cases the maximum shaft resistance of the pile τ_{rz} is also proportional to M.

ii) The variations of σ'_r with pile displacement are very similar for both analyses. They are not, therefore, strongly influenced by M.

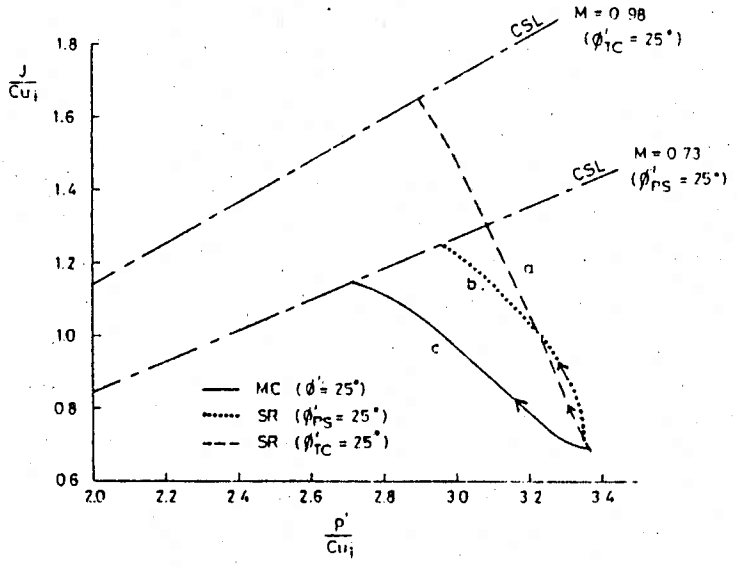

Figure 11: Stress paths as a function of the shape of the yield curve in the deviatoric plane

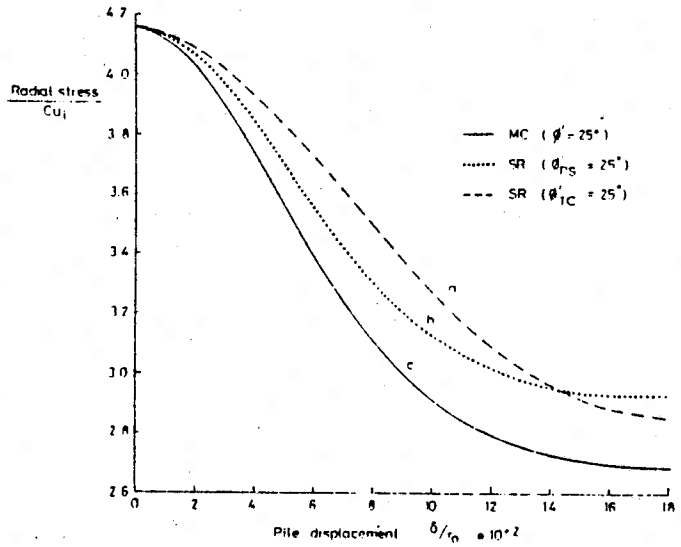

Figure 12: Variation of the radial stress as a function of the shape of the yield surface in the deviatoric plane

The results of the analysis using the Mohr Coulomb hexagon are indicated by the lines, labelled c, in figures 11 and 12. Inspection of figure 11 indicates that at peak the value of J, and hence τ_{rz}, is less than predicted using a surface of revolution for the shape of the yield surface in the deviatoric plane. A slightly larger reduction in σ'_r is also predicted, see figure 12. These observations indicate that analyses based on a soil model involving rotational symmetry about the space diagonal in effective stress space may lead to slightly unconservative predictions. However, it should be noted that the differences between the two analyses with the same $\phi' = 25^o$ at "plane strain", i.e. curves b and c, are at the most only 10% and therefore within the uncertainty arising from the selection of material parameters. Use of a surface of revolution for the shape of the yield surface therefore appears a reasonable approximation as long as the predicted shaft capacities are adjusted to give the appropriate M value at "plane strain" ($\theta = 0^o$). The predicted reduction in σ'_r needs no such adjustment.

ii) Initial Stress Ratio

One of the major conclusions arising from the work of Randolph et.al. (1979) is that immediately adjacent to the pile shaft the soil is in a normally consolidated condition after driving and subsequent pore pressure dissipation, the stresses being such that $\sigma'_z = \sigma'_\theta = K_{o_{nc}} . \sigma'_r$, where $K_{o_{nc}}$ is the "at rest" earth pressure coefficient appropriate to normally consolidated clay. For the situation of the pile installed in London clay discussed previously a $K_{o_{nc}}$ of 0.715 has been predicted. While this value is appropriate to the Modified Cam clay model it is not in agreement with Jaky's formula, $K_o = 1 - \sin\phi'$, which predicts a value of 0.5774. To investigate the likely effect of the magnitude of $K_{o_{nc}}$ on subsequent pile loading several analyses varying the value of this parameter have been performed. In all cases a Mohr Coulomb hexagon has been adopted for the shape of the yield surface in the deviatoric plane ($\phi' = 25^o$), and the undrained shear strength in plane strain C_{u_i} prior to pile loading has been set to a common value. Values of $K_{o_{nc}}$ of 0.715, 0.5774, and 0.6254 have been

adopted. The first of these corresponds to the situation predicted by Randolph et al (1979), where as the second is based on Jaky's formulae with a $\phi = 25^{\circ}$. The third value is also based on Jaky's formulae but with a $\phi = 22^{\circ}$ and represents the situation in which $\phi = 22^{\circ}$ in triaxial compression and 25° at "plane strain".

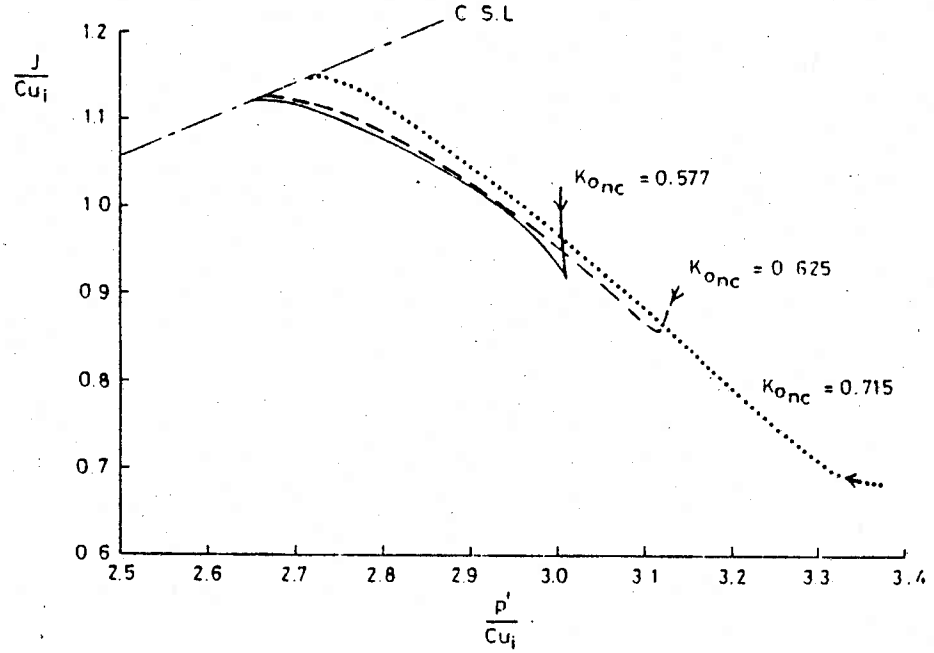

Figure 13: Stress paths as a function of initial stress ratio

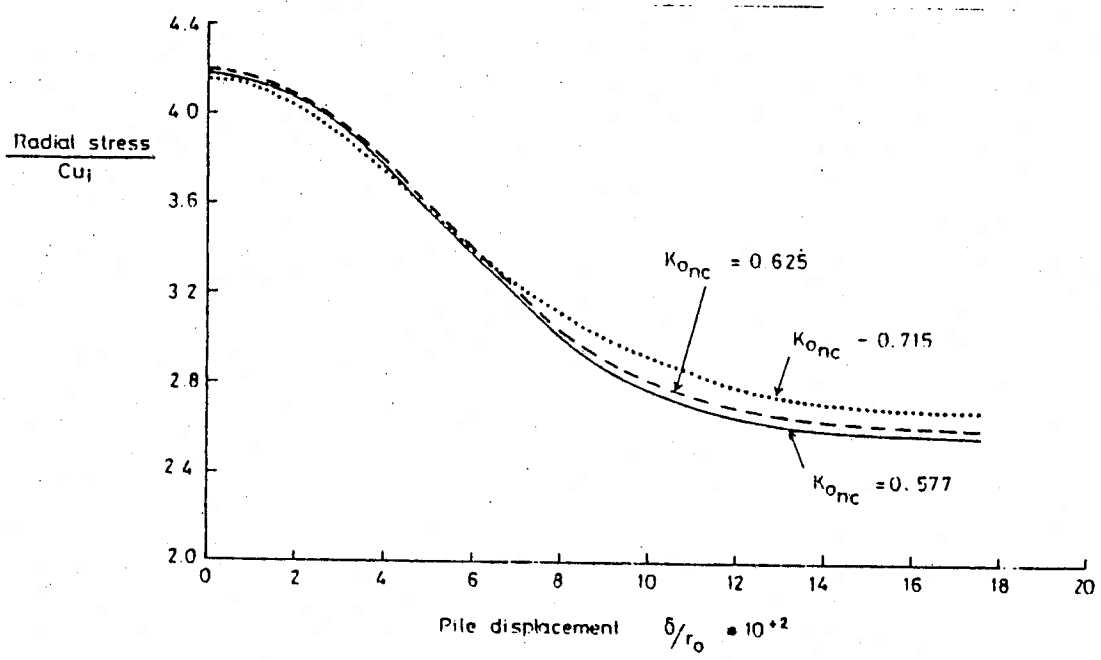

Figure 14: Variation of radial stress as a function of initial stress ratio

The predicted stress paths are presented in figure 13 and the reductions of σ'_r with pile displacement are shown in figure 14. Inspection of these plots indicate that the predicted value of J at peak (and therefore shaft friction τ_{rz}), and the changes in σ'_r are all very similar. This clearly indicates that the predictions are not greatly affected by the numerical value of Ko_{nc}, at least over the range considered.

iii) Initial Over Consolidation Ratio Adjacent to the Pile

As stated previously the cavity expansion theory predicts that the soil immediately adjacent to the pile shaft will always be in a normally consolidated condition after driving and subsequent pore pressure dissipation irrespective of the overconsolidation ratio in the soil prior to pile installation. In order to investigate the influence on loading of deviations from normal consolidation immediately adjacent to the pile two analyses with OCR's of 1.5 and 2 (defined as p_o/p') have been performed. The results of these calculations, in the form of stress paths and the reduction of σ'_r with pile displacement, are compared with the normally consolidated situation in figures 15 and 16 (solid lines).

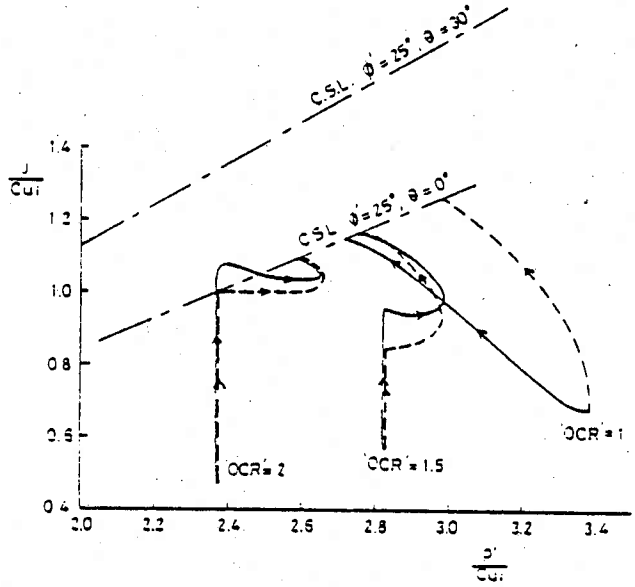

Figure 15: Stress paths as function of the over consolidation ratio adjacent to the pile

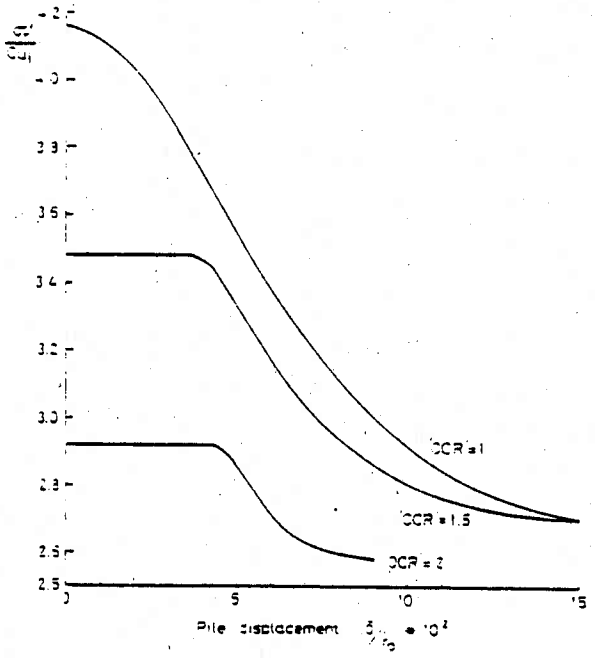

Figure 16: Variation of radial stress as a function of the over consolidation ratio adjacent to the pile

While there are clearly differences in these predictions, the values of J and σ'_r at peak loading are very similar for all cases. The stress conditions acting on the pile shaft at peak are therefore little affected by the actual OCR as long as the correct undrained strength after pile driving and pore pressure dissipation Cu_i has been defined. Corresponding results from analyses adopting a surface of revolution for the shape of the yield function in the deviatoric plane with a ϕ' value of 25^o in "plane strain" are shown as dotted lines in figure 15 for comparison.

6 SUMMARY AND CONCLUSIONS

A numerical study of the behaviour of driven piles on axial loading has been performed, employing a work hardening/softening elastoplastic constitutive law for the soil. The stress conditions induced around the pile as a result of installation were taken from predictions based on cavity expansion theory. The effects of deviations from these conditions were then examined with the aim of highlighting the features of the post-installation stress state which need to be determined with the greatest confidence.

It has been shown that the capacity of a pile loaded under drained conditions seldom exceeds that of one loaded under undrained conditions by more than about ten per-cent. A significant reduction in the radial effective stress on loading is predicted in both drained and undrained conditions; the peak mobilized angle of shaft friction was shown to be independant of the initial stress conditions ($\delta' = \tan^{-1}(\sin \phi')$).

It was demonstrated that the stress state in the soil closest to the pile has an over-riding influence on the loading behaviour, and that the conditions in the soil further away are relatively unimportant and therefore need not be predicted with great precision. To obtain the stress conditions immediately adjacent to the pile shaft from the cavity expansion calculations extrapolation is necessary, see Randolph et.al. (1979). As the stresses have highly varying gradients in this vicinity such extrapolation will be subject to error. Care must therefore be exercised when obtaining the initial stress conditions from the results of cavity expansion calculations.

A parametric study showed that provided the post installation undrained shear strength in the soil adjacent to the pile is correctly predicted, then the pile capacity is relatively insensitive to the ratio of stresses, the shape of the yield surface in the deviatoric plane, or the local overconsolidation ratio.

An approach commonly adopted in practice for the design of piles is to relate the unit shaft resistance to the undrained shear strength of the soil Cu_o prior to pile installation using the following empirical equation;

$$\tau_{Shaft} = \bar{\alpha} . Cu_o$$

where $\bar{\alpha}$ is an empirical constant. As the drained capacity is always predicted to be of the same order as the undrained capacity, values of $\bar{\alpha}$ in excess of unity are predicted from the analyses presented in this paper. This arises because the cavity expansion calculations used predict that the undrained strength post pile installation is greater than that before installation. In practice, values of $\bar{\alpha}$ are seldom above unity and it is believed that although there are many

contributing factors, a major reason for the discrepancy is the failure to take account of the severe fabric disturbance that must occur around a pile on driving. This is particularly applicable to soils with a high plasticity index. Work at Imperial College is currently in progress to quantify the effects of such fabric disturbance.

ACKNOWLEDGEMENTS

The writers are indebted to their colleagues at Imperial College, particularly Mr. A. Gens, for many stimulating discussions and considerable assistance; special thanks go to Professor J. B. Burland for his assistance and continuing encouragement. Mr. Martins was supported by an award from the Science Research Council.

REFERENCES

Chandler, R. J. and Martins, J. P. (1982).
An experimental study of skin friction around piles. Submitted for publication.

Kirby, R. C. and Esrig, M. I. (1980).
Further developments of a general effective stress method for prediction of axial capacity for driven piles in clay. Recent developments in design and construction of piles. I.C.E. London.

Potts, D. M. and Gens, A. (1982).
The analysis of boundary value problems in Geomechanics - the effect of the shape of the plastic potential. In preparation.

Potts, D. M. and Martins, J. P. (1982).
The shear resistance of axially loaded piles in clay - a theoretical study. Submited for publication.

Randolph, M. F., Carter, J. P. and Wroth, C. P. (1979).
Driven piles in clay - the effects of installation and subsequent consolidation. Geotechnique 29, no.4, 361-393.

Roscoe, K. H. and Burland, J. B. (1968).
On the generalised stress strain behaviour of 'wet' clays. Engineering plasticity, ed. J. Heyman and F. Leckie, 535-609, Cambridge, Cambridge University Press.

Wroth, C. P., Carter, J. P. and Randolph, M. F. (1980).
Stress changes around a pile driven into cohesive soil. Recent developments in the design and construction of piles. I.C.E, London